International Journal of Minerals, Metallurgy and Materials
Volume 18, Number 3, June 2011, Page 260
DOI: 10.1007/s12613-011-0432-y

UV/visible spectroscopic analysis of Co^{3+} and Co^{2+} during the dissolution of cobalt from mixed Co-Cu oxidized ores

J. Ndalamo[1)], *A.F. Mulaba-Bafubiandi*[2)], *and B.B. Mamba*[1)]

1) Department of Chemical Technology, University of Johannesburg, P.O. Box 17011, Doornfontein 2028, South Africa
2) Department of Extraction Metallurgy, University of Johannesburg, P.O. Box 17011, Doornfontein 2028, South Africa
(Received: 6 May 2010; revised: 12 June 2010; accepted: 26 June 2010)

Abstract: The leaching of cobalt from four-mixed Co-Cu oxidized ores containing cobalt at levels ranging from 0.5wt% to 34wt% was studied and the results has been reported. Conventional dissolution of these oxidized Co-Cu ores with diluted H_2SO_4 and SO_2 as a reducing agent resulted in a substantial improvement in the solution based recovery of cobalt. UV/visible spectroscopic analysis of the leached solutions indicated that the increased cobalt content in the solution was a result of flushing the acidified cobalt leaching solution with SO_2. Furthermore, UV/visible spectroscopy confirmed that as SO_2 was flushed into the acidified leaching solution, Co^{3+} bearing minerals were reduced to the readily soluble Co^{2+} bearing minerals, and this resulted in the increase of total cobalt in the collected solution. The mechanism of the reduction of Co^{3+} to Co^{2+} bearing minerals when SO_2 is flushed during the leaching of mixed Co-Cu oxidized ores, including the stability trends of Co^{3+}, Co^{2+}, and Cu^{2+} complexes, as shown by their UV/visible spectra, are also discussed.

Keywords: cobalt metallurgy; dissolution; leaching; reaction kinetics; spectroscopic analysis

1. Introduction

World-wide production of cobalt derives mainly as a by product from the extraction of other metals. Commercially important ores that contain cobalt include cobaltite (CoAsS), smaltite ($CoAs_2$), and linnaeite (Co_3S_4). These ores always occur together with nickel ores, often with copper ores and sometimes with lead ores. The pretreatment of these ores involves roasting, which converts the ore into a mixture of oxides called "Speisses". These oxides usually contain cobalt as Co^{3+} and Co^{2+} bearing minerals, and SO_2 is released as a valuable byproduct. Upon preconcentration, these oxides are treated with H_2SO_4, which dissolves cobalt and nickel, thereby separating them from copper [1].

Mixed Co-Cu oxidized ores that originate from the Democratic Republic of Congo (DRC) contain cobalt (mainly as Co^{3+}) at variable levels [2]. A detailed study of heterogenite samples from the southern Katanga region by Deliens and Goethals [3] revealed the existence of a heterogenite possessing a polytypic relation. This heterogenite, which was named "heterogenite-2H", was found to possess the same properties (except X-ray powder diffraction patterns) and chemical composition as the "normal" heterogenite. In order to distinguish it from the 2H polytype, the "normal" heterogenite was named the heterogenite-3R. In addition to being the most commonly found heterogenite in southern Katanga, the heterogenite-3R occurs with the widest range of appearances. The chemical formula of the "normal" heterogenite (CoO(OH)-3R) is identical to that of the heterogenite-2H (CoO(OH)-3H). The clearest distinction between the two polytypes is the 2H polytype rarity in comparison to the 3R, which is almost always present in the oxidation zones of the Cu-Co deposits in southern Katanga [3].

It has been reported that challenges are encountered during the dissolution of cobalt from these types of ores. Literature survey indicates that various reagents including copper powder (Cu), sodium metabisulphite ($Na_2S_2O_5$), and ferrous ions (Fe^{2+}) have been used as reducing agents in plant situations to improve the solubility of cobalt from such ores. However, it was also indicated that the use of these

Corresponding author: B.B. Mamba E-mail: bmamba@uj.ac.za

reagents resulted in an unbearable increase in total plant operation costs, where the consumption of these reagents averaged 0.8 t of $Na_2S_2O_5$ and 1.2 t of Cu powder per ton of dissolved cobalt, representing approximately 47% of the total operating cost per ton of Co metal produced [4].

Other studies have reported the use of sulphur dioxide (SO_2) as a reducing agent in improving the dissolution efficiency of cobalt from mixed Co-Cu oxidized ores [5-9]. These studies showed that a substantial improvement in the cobalt yield was achieved when the ores were leached in the presence of SO_2. This paper, therefore, reports on the mechanistic pathways of cobalt dissolution from mixed Co-Cu oxidized ores when SO_2 was used as a reducing agent. More emphasis has been placed on using UV/visible spectroscopy in trying to understand the solubility of Co^{3+} and Co^{2+} bearing minerals from mixed Co-Cu oxidized ores in the presence of SO_2. In conjunction to this, the dissolution kinetics of cobalt from mixed Co-Cu oxidized ores in admixtures of SO_2 is reported in this paper.

The important oxidation states of cobalt in aqueous solutions are Co^{3+} (d^6) and Co^{2+} (d^7) [10]. The fact that Co^{3+} forms an enormous number of octahedral complexes having the t_{2g}^6 configuration has resulted in these being used extensively for rate and mechanistic studies on octahedral substitution reactions. Co^{2+} forms more tetrahedral complexes than any other transition metal ions. The nature of the ligand bonded to cobalt has a dramatic effect on the stability of these two oxidation states [11]. Co^{3+} has a great affinity for nitrogen donors especially ammonia, amines, nitro (NO_2^-), and –NCS groups. Unlike cobalt, copper exist mainly as Cu^{2+} (d^9) in aqueous solution. Its d^9 configuration gives rise to Jahn-Teller distortions both in its simple compounds and complexes.

The valence-bond approach to bonding in complexes was first proposed by Lewis in 1902. It was not until 1927, however, that Walter Heitler and Fritz London showed how the sharing of electrons holds a covalent molecule together [12]. The last major step in the evolution of this theory was the suggestion by Linus Pauling that atomic orbitals mix to form hybrid orbitals, such as the sp, sp^2, sp^3, dsp^3, and d^2sp^3 orbitals. At almost the same time that these chemists were developing the valence-bond model for coordination complexes, while physicists, such as Hans Bethe, John Van Vleck, and Leslie Orgel, were developing an alternative theory known as the crystal field theory [13-16]. This theory tried to describe the effect of the electrical field of neighboring ions on the energies of the valence orbitals of an ion in a crystal. Both theories have been used in this study to explain the UV/visible absorption trends observed for Co^{3+}, Co^{2+}, and Cu^{2+} complexes.

2. Experimental procedure

2.1. Materials

The hand-picked preconcentrated mixed Co-Cu oxidized ores used in this study were obtained from DRC. These are high cobalt ore, high copper ore, low cobalt ore (with mica), and low cobalt ore (without mica), which were processed as received. The cobalt content in these ores ranged from 0.5wt% to 34wt% with the major constituents among other things being copper and iron. The cobalt phases in these ores were characterized by X-ray diffraction (XRD). Unless otherwise stated, all experiments were carried out at room temperature using reagent grade chemicals that were obtained at high purity from the suppliers.

2.2. Characterization by XRD

The powder sample (10 g) was finely ground in an agate mortar prior to XRD analysis. The sample for XRD analysis was prepared by packing the finely ground powder into a steel holder backed by a stainless steel slide, and this powder was then smoothed off by sliding a flat steel over the surface. The holder was slightly overfilled with the powder which was then compressed so that it could pack adequately onto the steel holder. The powder samples were analyzed with a computer-controlled Phillips diffractometer, type PW3710, with an automatic divergence slit and a copper anode producing X-rays of λ_1=0.1.5406 and λ_2=0.154443 nm. The diffractometer was operated at 40 kV and 40 mA, and automatic routines allowed absolute scanning for values of 2θ from 3 to 80°, using a step-size of 0.0170° and a scan step time of 49.2601 s. Identification and attribution of mineral phases in the ores was achieved with the aid of the Xpert computerized database.

2.3. Dissolution of cobalt from mixed Co-Cu oxidized ores

The main apparatus for the experiment consisted of a glass beaker (500 cm^3), a magnetic stirrer, and a pH/Eh meter. Buffer solutions of pH 4 and pH 7 were used to calibrate the pH probe. The ore sample (20 g) with a particle size distribution of less than 75 μm was poured into a glass beaker (500 cm^3) and charged with H_2SO_4 (400 cm^3, 0.5 M). H_2SO_3 was produced, when necessary, by purging a glass beaker (500 cm^3) charged with deionized water (400 cm^3) with SO_2 at a flow rate of 50 cm^3/min. The residence time for all experiments was 2 h. The magnetic stirrer was set at 300

r/min, and the flow rate of SO_2 gas was monitored with the help of calibrated bubble flow meters. Samples were collected at 30-min time intervals and analyzed for cobalt by flame-AAS.

2.4. Analysis of Co^{3+}, Co^{2+}, and Cu^{2+} by UV/visible spectroscopy

All ultraviolet (UV/visible) experiments were performed using a Varian UV/visible Carry 50 spectrophotometer and a 10-mm quartz cuvette cell. The UV/visible experiments were carried out to monitor the levels of Co^{3+} and Co^{2+} in the ore prior to leaching and in residues after the leaching of mixed Co-Cu oxidized ores. In a typical experiment, a finely ground ore or residue sample (0.2 g) with a particle size of less than 75 μm was dissolved in aqua-regia (40 mL) and heated on a hot plate for 10 min. The resulting solution was cooled and transferred to 250-mL volumetric flask. A solution of 2 M ammonium thiocyanate (NH_4SCN) was then added as a diluent, together with a chromogenic (color forming) reagent in order to convert the cobalt species to absorbing complex forms. Qualitative analysis was immediately carried out by scanning aliquots of this solution on a Varian UV/Visible Carry 50 spectrophotometer. The absorbance spectra of both Co^{3+} and Co^{2+} complexes were collected from 190 to 900 nm. Furthermore, a synthetic solution containing Co^{3+}, Co^{2+}, and Cu^{2+} was prepared at similar concentration levels as in the sample and analyzed in the same manner.

3. Results and discussion

3.1. Analysis of mixed Co-Cu oxidized ores by XRD

The XRD diffraction patterns shown in Fig. 1 indicate the chemical composition of cobalt in three different cobalt-bearing ores, namely, high cobalt ore—CoOOH-3R (Fig. 1(a)), high copper ore—CoOOH-3R (Fig. 1(b)), and low cobalt ore (without mica)—CoOOH-3R and CoOOH-2H (Fig. 1(c)). Since the sulphur content in these ores was not analyzed, it was assumed that the mixed Co-Cu ores were completely oxidized. The attribution of mineral phases, as shown in Fig. 1, was achieved by comparing the principal peak intensities to reference XRD cards.

Heterogenite (CoOOH), malachite ($Cu_2(CO_3)(OH)_2$ and limonite ($Fe_2O_3 \cdot 3H_2O$) were identified as common phases in all four mixed Co-Cu oxidized ores. Nimite-$1M_{11b}$ [$(Ni, Mg, Al)_6(Si, Al)_6O_{10}(OH)_8$] and willemseite [$(Ni, Mg)_3Si_4O_{10}(OH)_2$] were also identified as commonly occurring minerals which contain nickel. In addition, two forms of heterogenite minerals were identified in the low cobalt ores, that is, heterogenite-2H (CoOOH-2H) and heterogenite-3R (CoOOH-3R). As a general comment, it was noted that XRD failed to detect any Co^{2+}-bearing minerals in all of the four mixed Co-Cu oxidized ores being investigated. It was suspected that this was caused by the low detection limit (3%) of the XRD instrument used in this study. Further experiments still need to be conducted to clarify this matter.

The XRD analysis provided evidence that the mixed Co-Cu oxidized ores contained both the Co^{3+} bearing mineral (heterogenite) and the Cu^{2+} bearing mineral (malachite). This facilitated the investigation and understanding of the aqueous chemistry of cobalt and copper before and after dissolution experiments.

The results shown in Table 1 summarizes the mineral phases derived from the mineralogical studies of all four mixed Co-Cu oxidized ores by XRD. The percentage (%) match score or percentage modal in Table 1 refers to the relative match factor with the data given in the XRD mineral powder diffraction data base. As can be noted in Table 1, the ratio of silica (SiO_2) to iron (Fe) content is high in all four ores. Willemseite was identified as a nickel containing mineral in the high copper ore instead of nimite, which appears to be common in the other three ores. It can also be noted that the minerals identified for the low cobalt ores with and without mica are identical in all proportions. This implies that the presence of mica in the low cobalt ore does not affect the crystal structure of minerals in the ore. It has yet to be ascertained whether the presence of mica had any effect on the leaching efficiency of cobalt from the low cobalt bearing ores.

3.2. Dissolution of cobalt from mixed Co-Cu oxidized ores

Fig. 2(a) shows that the rate of cobalt dissolution from the high cobalt ore initially accelerates and reaches a plateau after leaching for 30 min. After 30 min, the leaching rate becomes progressively slower until the reaction reaches completion. This trend is observed for all the leaching reagents investigated. Leaching with H_2SO_4+SO_2, H_2SO_3, and SO_2+H_2O achieves cobalt dissolutions as high as 80% to 98%. When aqueous H_2SO_4 is used as the leaching reagent, only 10% Co dissolution is achieved. In general, it can be inferred from Fig. 2 that the extent of Co dissolution is high when admixtures of H_2SO_4+SO_2 are used as the leaching media, instead of aqueous H_2SO_4 alone.

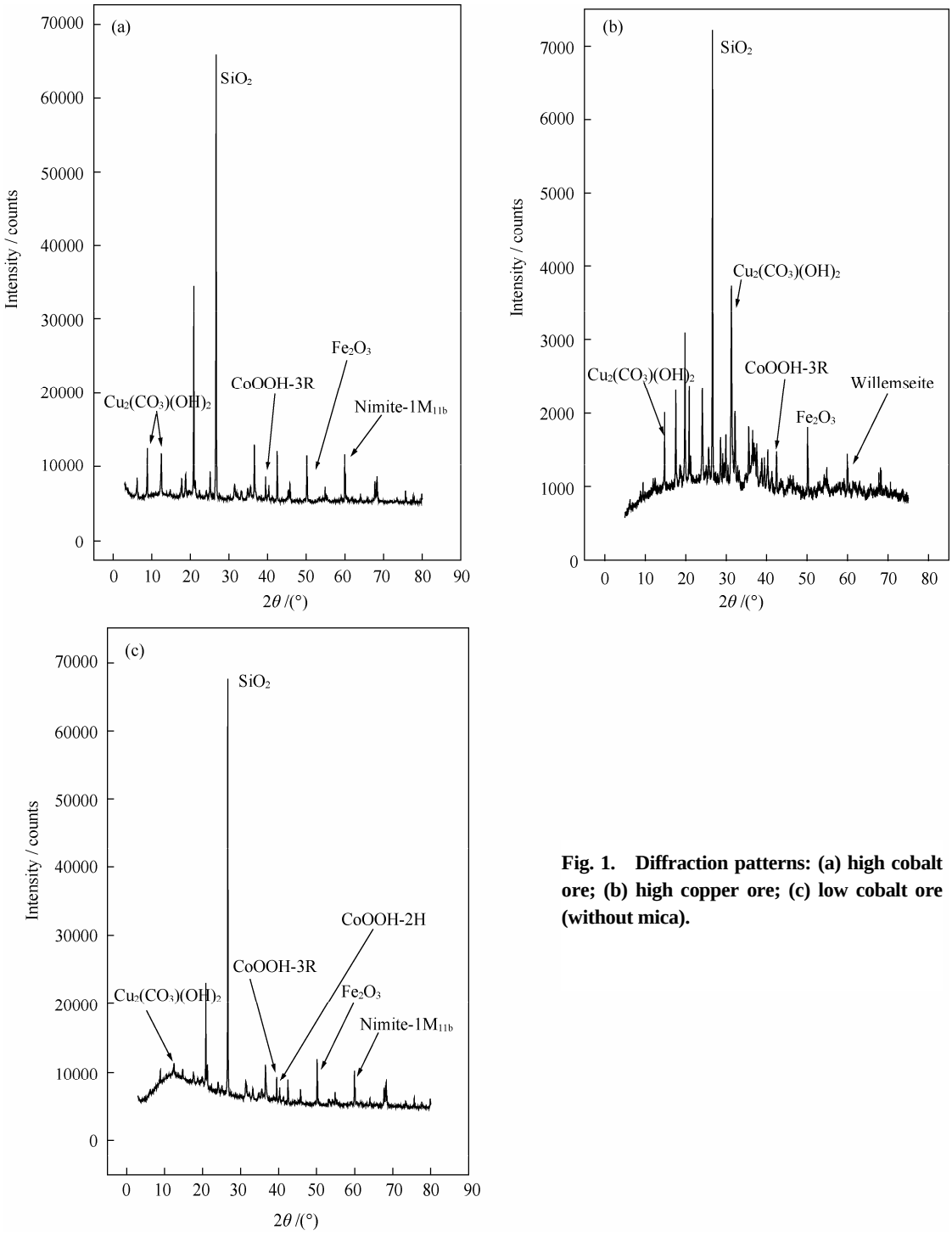

Fig. 1. Diffraction patterns: (a) high cobalt ore; (b) high copper ore; (c) low cobalt ore (without mica).

The extent of Co dissolution with respect to the high copper ore, as shown in Fig. 2(b), is found to be relatively lower than that in Fig. 2(a), reaching a maximum of 80%. In comparison, it is observed that the leaching behavior of cobalt from the high copper ore (0.499wt% Co) follows similar leaching trends as observed in the high cobalt ore (34.2wt% Co) but at a slower leaching rate. That is, more time is required to leach cobalt from a low cobalt bearing ore (*i.e.*, high copper ore) than from a high cobalt bearing ore (*i.e.*, high cobalt ore).

The kinetic curves shown in Figs. 2(c) and 2(d) also show an elevated initial rate of cobalt leaching within the first 30 min, which levels out beyond 30 min. It is also noted that a maximum of Co dissolutions from the low cobalt ore

Table 1. Identification of mineral phases in mixed Co-Cu ores by XRD

High cobalt ore		High copper ore	
Mineral phase	Match score / %	Mineral phase	Match score / %
SiO_2	64	SiO_2	76
CoOOH-3R	22	CoOOH-3R	11
$Cu_2(CO_3)(OH)_2$	17	$Cu_2(CO_3)(OH)_2$	41
Fe_2O_3	13	Fe_2O_3	23
Nimite-1M_{11b}	10	Willemseite	10

Low cobalt ore with mica		Low cobalt ore without mica	
Mineral phase	Match score / %	Mineral phase	Match score / %
SiO_2	56	SiO_2	59
CoOOH-2H	5	CoOOH-2H	4
CoOOH-3R	11	CoOOH-3R	8
$Cu_2(CO_3)(OH)_2$	19	$Cu_2(CO_3)(OH)_2$	16
Fe_2O_3	12	Fe_2O_3	11
Nimite-1M_{11b}	11	Nimite-1M_{11b}	10

with mica (3.963wt% Co) and the low cobalt ore without mica (2.806wt% Co) are achieved by leaching with admixtures of the two acids. The results obtained for leaching cobalt from both the low cobalt bearing ores are similar, indicating that the presence of mica does not affect the leaching efficiency of Co, since the dissolution efficiency remains the same in both cases. In general, high cobalt yields are achieved when admixtures of SO_2 and H_2SO_4 are used as the leaching reagent.

According to the trends in Fig. 2, there was a need to elucidate and understand the role of SO_2 in leaching cobalt from mixed Co-Cu oxidised ores, where SO_2 was obtained as the anhydride of sulphurous acid.

$$SO_{2(g)} + H_2O_{(l)} \Leftrightarrow H_2SO_{3(aq)} \quad (1)$$

The sulphurous acid produced by reaction (1) is unstable with the reverse reaction being favored. The corresponding anions are bisulphite (HSO_3^-) and sulphite (SO_3^{2-}). Sulphur dioxide can serve as either a reducing agent or as an oxidizing agent, although the former is its more usual role.

The role of SO_2 as a reducing agent was applied during the leaching of mixed Co-Cu oxidized ores that bear cobalt mainly as Co^{3+} (CoOOH) as evidenced by the mineralogical studies. SO_2 in this case reduces Co^{3+} to Co^{2+}, as shown in reaction (2):

$$SO_{3(aq)}^{2-} + 2Co_{(aq)}^{3+} + H_2O \rightarrow SO_{4(aq)}^{2-} + 2Co_{(aq)}^{2+} + 2H_{(aq)}^{+} \quad (2)$$

In contrast, sulphuric acid ($H_2SO_{4(aq)}$) is diprotic; the first dissociation is strong, and the second is moderately strong (K_2=1.1×10^{-2}). The sulphate anion (SO_4^{2-}) has a tetrahedral geometry. The S–O bond length is 0.151 nm, which is quite small compared with the value predicted from the sum of the sulphur and oxygen single-bonded radii (0.170 nm). This indicates that the bond in SO_4^{2-} has a substantial double bond character. Double bonds can form by the overlapping of the 2p orbitals on the oxygen atoms with the 3d orbitals on the sulphur atom. Therefore, not only is sulphuric acid a powerful dehydrating agent but also a very strong leaching agent.

The role of sulphuric acid as a strong leaching agent is illustrated below:

$$CuO_{(s)} + H_2SO_{4(aq)} \rightarrow CuSO_{4(aq)} + H_2O_{(l)} \quad (3)$$

$$CoO_{(s)} + H_2SO_{4(aq)} \rightarrow CoSO_{4(aq)} + H_2O_{(l)} \quad (4)$$

In view of the above, the leaching pathways in reactions (5) to (7) show the dissolution behavior of cobalt from mixed Co-Cu oxidized ores from a chemistry perspective. These mechanistic pathways elucidate the role of SO_2 and H_2SO_4 during the leaching process. As indicated in the mineralogical studies of mixed Co-Cu oxidized ores, the mineral Co_3O_4 can also be written as $CoO \cdot Co_2O_3$, which clearly denotes Co^{2+} and Co^{3+} forms, that is, CoO bears Co^{2+} and Co_2O_3 bears Co^{3+}. Since it was observed that Co^{3+} bearing minerals are not directly soluble in acid, the dissolution of cobalt from Co_3O_4 mineral is shown in the reaction schemes below:

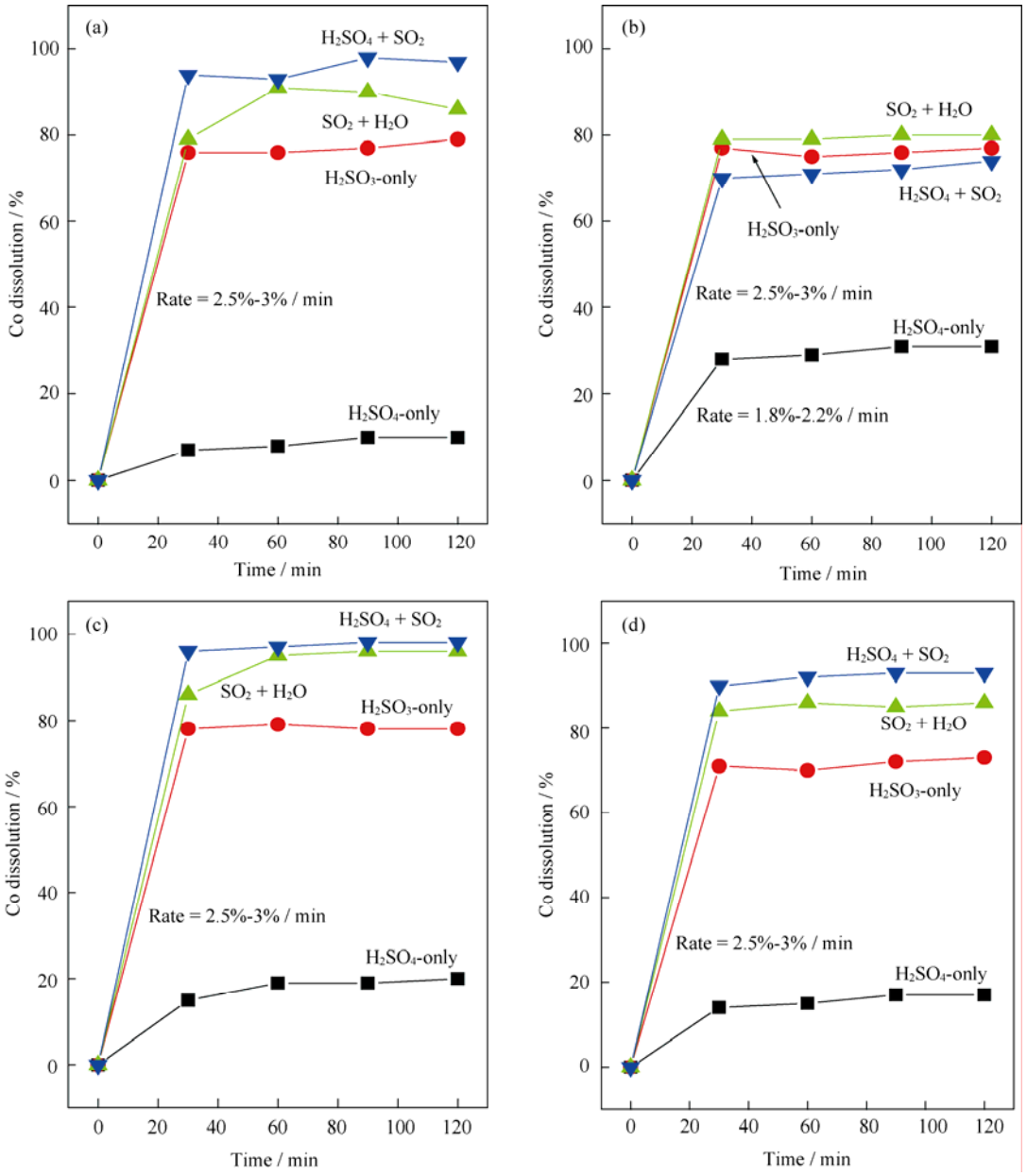

Fig. 2. Leaching behaviour of cobalt: (a) high cobalt ore; (b) high copper ore; (c) low cobalt ore with mica; (d) low cobalt ore without mica.

$$CoO{\cdot}Co_2O_{3(s)} + H_2SO_{4(aq)} \rightarrow CoSO_{4(aq)} + Co_2O_3{\cdot}H_2O_{(s)} \quad (5)$$

$$SO_{2(g)} + H_2O_{(l)} \longrightarrow$$

$$Co_2O_3{\cdot}H_2O_{(s)} + H_2SO_{3(aq)} \rightarrow CoO_{(s)} + H_2O_{(l)} \quad (6)$$

$$CoO_{(s)} + H_2SO_{4(aq)} \rightarrow CoSO_{4(aq)} + H_2O_{(l)} \quad (7)$$

Reaction (5) illustrates the dissolution of Co from $CoO{\cdot}Co_2O_3$, and one of the products is $Co_2O_3{\cdot}H_2O$, which is simply a hydrated form of Co_2O_3. It can be noted that $Co_2O_3{\cdot}H_2O$ bears Co as Co^{3+} in reaction (5), and thus, most of the cobalt recovered as $CoSO_4$ in reaction (6) comes from CoO. Reaction (6) illustrates a situation whereby SO_2 also forms part of the leaching solution, that is, reaction (6) is a continuation of reaction (6). Here, SO_2 is flushed into the acidified cobalt leaching solution. As seen in reaction (6), H_2SO_3 reduces $Co_2O_3{\cdot}H_2O$ (product from reaction (5)) to CoO, which is directly soluble in H_2SO_4. Reaction (7) illustrates how easily the dissolution of Co from CoO can be and how crucial it is to incorporate a reduction step (using SO_2) during the leaching of mixed Co-Cu oxidized ores.

3.3. Analysis of Co^{3+} and Co^{2+} by UV/visible spectroscopy

In order to evaluate and confirm the reduction of Co^{3+} to Co^{2+} minerals by flushing SO_2 into the acidified leaching medium during the leaching process, the concentrations of Co^{3+} and Co^{2+} in ores before SO_2 treatment were determined by UV/visible spectroscopy. The absorbances of both Co^{3+} and Co^{2+} were plotted against the respective absorption wavelengths of Co^{3+} and Co^{2+}. The results for the levels of Co^{3+} and Co^{2+} before SO_2 treatment are shown in Fig. 3(a).

The mixed Co-Cu oxidized ores were then leached in aqueous H_2SO_4, while SO_2 was flushed into the leaching system. The leaching process was allowed to take place for 30 min and then stopped. The solution was filtered off, and the residue was analyzed for the concentrations of Co^{3+} and Co^{2+} by UV/visible spectroscopy. The absorbances of both Co^{3+} and Co^{2+} were again plotted against their respective absorption wavelengths, and this plot is labeled as "After SO_2 treatment" in Fig. 3(b).

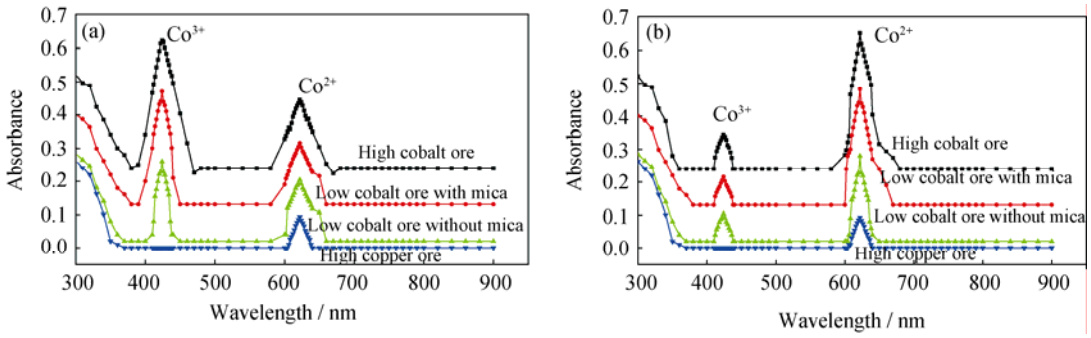

Fig. 3. UV/visible spectra of samples: (a) before SO_2 treatment; (b) after SO_2 treatment.

It can be seen from Fig. 3(a) that before SO_2 treatment, the concentration of Co^{3+} is greater than that of Co^{2+} in ores. After SO_2 treatment, in Fig. 3(b), the concentration of Co^{2+} in residue is greater than that of Co^{3+} in all the ores, with the exception of the high Cu bearing ore. Therefore, the role of SO_2 in reducing Co^{3+} to Co^{2+} minerals with subsequent improvement in the solution-based recovery of Co was clarified. The reason behind the stable trend in the Co^{2+} concentration observed with the high copper ore is not understood.

Fig. 4 illustrates the individual behavior of Co^{3+} and Co^{2+} in the individual ores before and after SO_2 treatment. It can also be noted in Fig. 4(a) that the absorbance of Co^{3+} before SO_2 treatment in the high cobalt ore is high compared with the absorbance of Co^{2+} before SO_2 treatment. The reverse trend is observed after leaching the high cobalt ore in the presence of SO_2. Here, the absorbance of Co^{3+} is smaller than that of Co^{2+}. Similar trends are observed in the case of low cobalt ores, with and without mica, in Figs. 4(b) and 4(c), respectively. This trend in the behavior of Co^{3+} and Co^{2+} shows a reduction in the concentration of Co^{3+} with an increase in Co^{2+} concentration as the mixed Co-Cu ores were leached in the presence of SO_2. The reasons for the behavior observed in Fig. 4(d) could not be explained. Further experiments still need to be carried out.

In general, higher yields of cobalt were achieved when leaching the mixed Co-Cu oxidized ores in the presence of SO_2. During the 2 h of leaching, it was noted that the maximum solution-based recovery of cobalt from these ores was achievable even within the first 30 min (Fig. 2) of leaching in admixtures of SO_2. It was therefore of interest to focus on the reduction of Co^{3+} to Co^{2+} within the first 30 min of leaching and determine the rate at which this was happening.

3.4. Analysis of Co^{3+}, Co^{2+}, and Cu^{2+} solution by UV/visible spectroscopy

The spectra shown in Fig. 5 illustrate the changes in absorption behavior of Co^{3+}, Co^{2+}, and Cu^{2+} before SO_2 treatment (Fig. 5(a)) and after SO_2 treatment ((Fig. 5(b)). The electron configuration of a neutral cobalt atom is Co: [Ar] $4s^2 3d^7$. The electron configurations for Co^{3+} and Co^{2+} complexes are Co^{3+}:[Ar] $3d^6$ and Co^{2+}:[Ar] $3d^7$. In general, the electrons are removed from the valence-shell s orbitals before they are removed from valence d orbitals when cobalt is ionized. The electron configuration of Cu^{2+} is Cu^{2+}:[Ar] $3d^9$. The valence bond theory with respect to Co^{3+} (d^6), in this case, suggests that having the six electrons in d_{xy}, d_{xz}, and d_{yz} orbitals leaves, $3d_{x^2-y^2}$, $3d_{z^2}$, 4s, $4p_x$, $4p_y$, and $4p_z$ unoccupied. These vacant orbitals mix to form a set of empty d^2sp^3 orbitals that point toward the corners of an octahedron. Each of these hybrid orbitals accepts a pair of electrons from a SCN^- ligand to form a complex in which the cobalt atom has a filled shell of valence electrons.

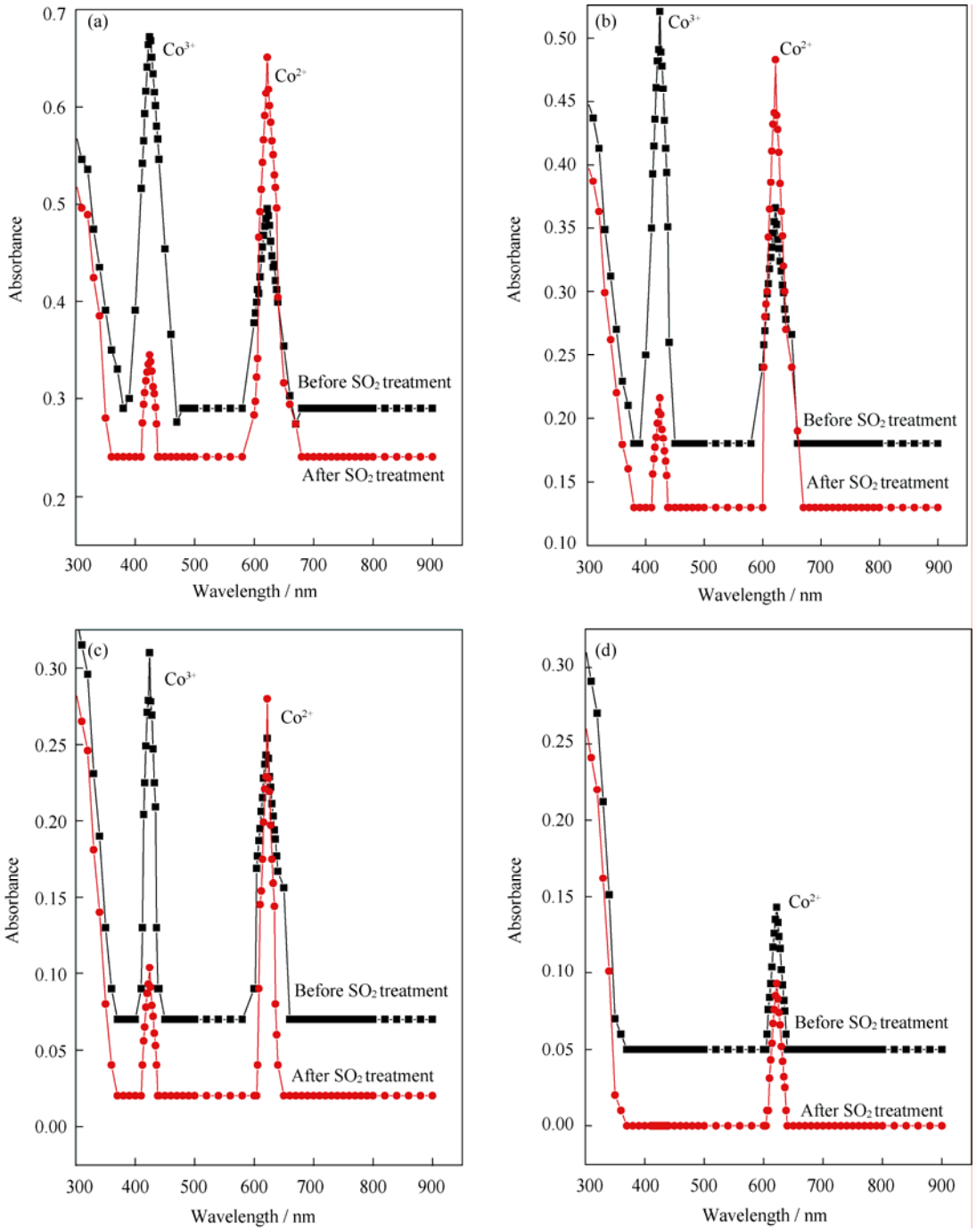

Fig. 4. UV/visible spectra for high cobalt ore (a), low cobalt with mica (b), low cobalt without mica (c), and high copper ore (d).

Co^{2+} (d^6) forms more tetrahedral complexes than any transition metal ions. The d_{z^2} and $d_{x^2-y^2}$ orbitals in this case do not point in the direction of the ligand charges and hence are at a lower energy than the d_{xy}, d_{xz}, and d_{yz} sets, which point more closely to the ligand positions. Unlike the situation in the octahedral case, in the tetrahedral field, none of the d orbitals points exactly at the ligands. The energy separation between two sets of orbitals is thus less than it was in the octahedral case (Co^{3+}). The splitting in the Co^{2+} tetrahedral case ($e^4t_{2g}^3$) is therefore inverted compared with that in the Co^{3+} octahedral case ($t_{2g}^6 e^0$). Therefore, Co^{2+} complexes are expected to absorb UV light at higher wavelengths (less energy) than Co^{3+} complexes with the same ligand. This is found experimentally to be the case (Fig. 5). This explains the electronic effects that contribute toward the stability of octahedral Co^{3+} as opposed to tetrahedral Co^{2+} ions.

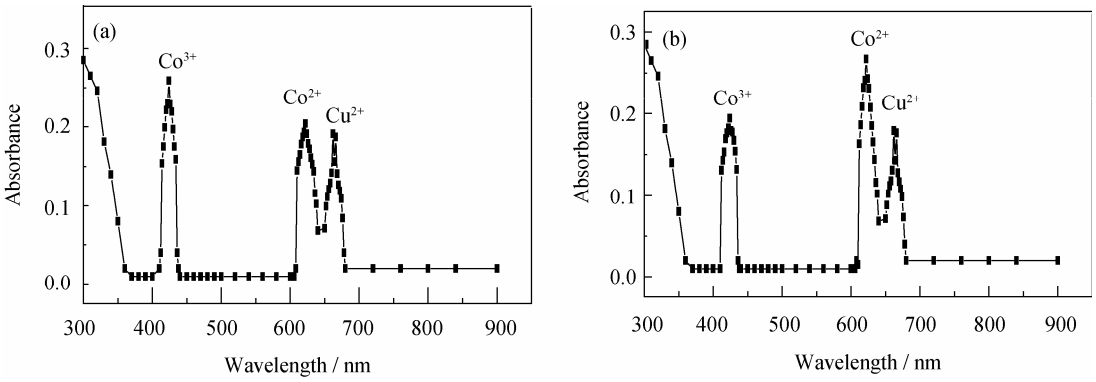

Fig. 5. UV/visible spectra for Co^{3+}, Co^{2+}, and Cu^{2+}: (a) before SO_2 treatment; (b) before SO_2 treatment.

A very important electronic effect of Cu^{2+} shows that, in many cases, these pure stereochemistries are distorted. This effect was first formulated by Jahn and Teller in 1937 (Jahn-Teller distortion). The Cu^{2+} (d^9) is the most stable oxidation state of copper in aqueous solution. Its d^9 configuration gives rise to Jahn-Teller distortions in complexes. In an octahedral field, Cu^{2+} has the electronic structure $t_{2g}^6 e^3$. Since the e_g levels are degenerate, either the d_{z^2} or $d_{x^2-y^2}$ orbital can be doubly filled. If the d_{z^2} orbital is doubly filled and the $d_{x^2-y^2}$ singly filled, the result of this orbital occupancy is that the ligands along the *x* and *y* axes are drawn closer to the copper ion. This is because electrons in the d_{z^2} orbital experience the electrostatic attraction of the Cu^{2+} ion more than the ligands do along the *z* axis, which are shielded from the Cu^{2+} ion by an extra electron in the $d_{x^2-y^2}$ subshell. The resulting structure has four short bonds (contraction along the *x* and the *y* axes) and two longer bonds (*z* axes) resulting in a tetragonal distortion. Because of this distortion the Cu^{2+} complex with an electron configuration of $t_{2g}^6 e^3$ (d^9) is energetically less stable than the tetrahedral Co^{2+} (d^7) complex and therefore absorbs UV light at a higher wavelength than Co^{2+}, as can be seen in Fig. 5.

4. Conclusion

XRD analysis successfully explored and confirmed the presence of cobalt, copper, and iron bearing minerals in all of the four mixed Co-Cu oxidized ores investigated. Although not much information pertaining to Co^{2+} bearing minerals in mixed Co-Cu oxidized ores was derived from the XRD results, heterogenite minerals (CoOOH-2H and CoOOH-3R) that bear cobalt as Co^{3+} were noted. Exceptional cobalt yields (*i.e.*, 85%-95% dissolutions) in the solution were achieved when the dissolution of mixed Co-Cu oxidized ores was carried out in the presence of SO_2. UV/Visible spectroscopic analysis of Co^{3+} and Co^{2+} before and after the dissolution experiments confirmed that improved cobalt yields using SO_2 as a reducing agent were due to the reduction of Co^{3+} to Co^{2+}.

Furthermore, the uncertainty around Co^{2+} and Cu^{2+} absorbing UV light at different wavelengths has been explained using the crystal field theory. In addition, one of Hund's rules states that the most stable oxidation state is the one with maximum multiplicity (n+1), where n is the number of unpaired electrons. It is therefore found that Co^{2+} (d^7) has three unpaired electrons in its t_{2g} subshell and Cu^{2+} (d^9) has only one unpaired in its e_g subshell. This gives Co^{2+} a total multiplicity of 4 and Cu^{2+} a multiplicity of 2. This further suggested that Co^{2+} is energetically more stable than Cu^{2+}.

References

[1] W. Zhang, P. Singh, and D. Muir, Oxidative precipitation of manganese with SO_2/O_2 and separation from cobalt and nickel, *Hydrometallurgy*, 63(2002), p.127.

[2] A.F. Mulaba-Bafubiandi, The effects of process parameters on the acid leachability of cobalt and related impurities from heterogenite ore from Katanga (DRC), [in] *Proceeding of SAIMM issue Base Metals Conference: Copper Cobalt Nickel and Zinc Recovery*, The South African Institute of Mining and Metallurgy, 2001, p.1.

[3] K.M. Deliens and H. Goethals, Polytypism of heterogenite, *Mineral. Mag*., 39(1973), p.152.

[4] K. Kongolo, M.D Mwema, A.N. Banza, and E. Gock, Cobalt and zinc recovery from copper sulphate solution by solvent extraction, *Miner. Eng.*, 16(2003), p.1371.

[5] J.A. Golding and Pushparajah, Mass transfer characteristics of cobalt and nickel in di(2-ethylhexyl) phosphoric acid under steady-state extraction conditions, *Hydrometallurgy*, 14(1985), p.295.

[6] R. Ebrahimi-Kahrizsangi, M.H. Abbasi, and A. Saidi, Molybdenite alkali fusion and leaching: reactions and mechanism, *Int. J. Miner. Metall. Mater*., 17(2010), No.2, p.127.

[7] H.P. Wang, J. Zhao, W. Liang, Y. Mei, B. Houdeh, and Y. Tian,

A new route of ferric ions rejection in a synthetic nickel leach solution, *Int. J. Miner. Metall. Mater*., 17(2010), No.3, p.257.

[8] N.V. Thakur and S.L. Mishra, Separation of Co, Ni and Cu by solvent extraction using di-(2-ethylhexyl) phosphonic acid, PC 88A, *Hydrometallurgy,* 48(1998), p.277.

[9] B. Ramachandra Reddy, D. Neela Priya, S. Venkateswara Rao, and P. Radhika, Solvent extraction and separation of Cd(II), Ni(II) and Co(II) from chloride leach liquors of spent Ni-Cd batteries using commercial organo-phosphorus extractants, *Hydrometallurgy*, 77(2005), p.253.

[10] I. Van de Voorde, L. Pinay, E. Courtjin, and F. Verport, Influence of acetate ions and the role of the diluents on extraction of Cu(II), Ni(II), Co(II), Mg(II) and Fe(II,III) with different types of extractants, *Hydrometallurgy*, 78(2005), p.92.

[11] A. Knowles and C. Burgess, *Practical Absorption Spectroscopy*, Vol.3, Chapman and Hall, London, 1984, p.1.

[12] F. Basolo and R. Johnson, *Co-ordination Chemistry*, Benjamin, New York, 1964, p.152.

[13] B.N. Figgis and J. Lewis, *Techniques of Inorganic Chemistry*, Vol.4, Interscience, New York, 1965, p.137.

[14] A.B.P. Lever, *Inorganic Electronic Spectroscopy*, Elsevier, Amsterdam, 1968, p.253.

[15] D. Sutton, *Electronic Spectra of Transition Metal Complexes*, McGraw-Hill, London, 1968, p.128.

[16] D. Benson, *Mechanisms of Inorganic Reactions in Solution*, McGraw-Hill, London, 1968, p.158.